AIP Advances

Optoelectronic performance of AgNW transparent conductive films with different width-to-height ratios and a figure of merit embodying an optical haze

Cite as: AIP Advances **9**, 045226 (2019); https://doi.org/10.1063/1.5081986
Submitted: 19 November 2018 . Accepted: 16 April 2019 . Published Online: 26 April 2019

A. Hubarevich, M. Marus, Y. Mukha, K. Wang, A. Smirnov, and X. W. Sun

Optoelectronic performance of AgNW transparent conductive films with different width-to-height ratios and a figure of merit embodying an optical haze

Cite as: AIP Advances 9, 045226 (2019); doi: 10.1063/1.5081986
Submitted: 19 November 2018 • Accepted: 16 April 2019 •
Published Online: 26 April 2019

View Online Export Citation CrossMark

A. Hubarevich,[1] M. Marus,[1,2] Y. Mukha,[1] K. Wang,[2,3] A. Smirnov,[1,a)] and X. W. Sun[2,3,b)]

AFFILIATIONS

[1] Laboratory for Information Displays and Optical Processing Systems, Belarusian State University of Informatics and Radioelectronics (BSUIR), 6 P. Brovki Street, Minsk 220013, Belarus

[2] Shenzhen Key Laboratory of Advanced Quantum Dot Displays and Lighting, Guangdong Higher Education Key Lab of Advanced Quantum Dot Displays and Lighting, and Department of Electrical & Electronic Engineering, Southern University of Science and Technology (SUSTech), 1088 Xueyuan Avenue, Shenzhen 518055, P.R. China

[3] Shenzhen Planck Innovation Technologies Co. Ltd, Shenzhen 518112, China

[a)] smirnov@bsuir.by
[b)] sunxw@sustc.edu.cn

ABSTRACT

Transparent conductive films (TCFs) based on rectangularly shaped silver nanowires (AgNWs) with different width-to-height ratios were theoretically studied. We show that tall AgNWs (height > width) possess higher transmittance and lower sheet resistance compared to other configurations of AgNWs. Moreover, tall AgNWs possesses significantly higher optical haze, which makes them a transparent conductor of choice for thin solar cell applications. For applications requiring low haze such as displays and touch screens, we propose an updated figure of merit embodying transmittance, sheet resistance and haze, allowing tuning width-to-height ratio to achieve a reasonable AgNW TCF performance trade-off. Obtained results offer a means for deeper analysis of AgNW properties for many optoelectronic applications.

I. INTRODUCTION

Transparent conductive films (TCFs) are a key component of many optoelectronic devices such as displays, solar cells, touch-screens, and light-emitting diodes.[1–8] Till date, indium tin oxide (ITO) based TCFs dominate an electronics industry.[9] But a high fabrication cost and inflexibility of the ITO prevent its application in future generation devices.[10–14] Among potential candidates (graphene, polymers, zinc oxide and other) to replace the ITO, silver nanowires (AgNWs) offer beneficial transmittance, sheet resistance, fabrication cost, flexibility and stretchability.[15–22]

Two main categories of AgNWs based on fabrication method are chemically synthesized NWs, randomly arranged on the substrate,[23,24] and uniform NW meshes made by various lithographical approaches.[25,26] Previous studies showed that the variation of AgNW thickness and surface coverage allow tuning not only the transmittance and sheet resistance, but also the ratio of scattered to total transmitted light – so-called optical haze.[27–29] Previous studies characterized the optical haze for AgNWs with square and circular cross-section, which thickness ranged from tens to hundreds of nanometers. For instance, AgNW TCFs with diameter below 50 nm possess low haze ~ 2%, vital to obtain displays with crystal-clear image.[30] Thicker AgNWs significantly increase the optical haze and improve an absorbance of thin film solar cells due to longer light pathway.[31]

Here we study other AgNW dimensions to deeper understand its influence on the transmittance, sheet resistance and haze. We investigate the rectangularly shaped AgNWs with various width-to-height ratio and demonstrate how these parameters affect AgNW performance. In addition, we update Haacke's figure of merit to enclose the optical haze, which offers a new glance on AgNW performance trade-off.

II. METHODOLOGY

We address the term *flat* AgNW films to the NWs with width exceeding the height or $w > h$, and the *tall* AgNW films to the NWs with height exceeding the width or w < h. Even though some of the structures discussed below are difficult to implement today, they possess interest for the next generation of optoelectronic applications. Figures 1 a) and b) shows the geometrical models for flat and tall AgNW films on glass substrate, respectively. Rectangularly shaped AgNWs were uniformly arranged across the substrate with the lattice constant *a*, height *h*, and width *w*. We range h and w from 30 to 500 nm and NW surface coverage SC from 5 to 50% to investigate AgNW performance in the nano- and microscale regions.

A commercial-grade simulator based on the finite-difference time-domain (FDTD) method was used to perform the optical calculations.[32] The material index of refraction and extinction coefficient was taken from Ref. 33. The incident light in the visible wavelength range from 400 to 700 nm was illuminated along Z axis. The periodic boundary conditions and perfectly matched layers were applied perpendicular and parallel to Z axis, respectively, and the simulation unit cell was set to a^2.

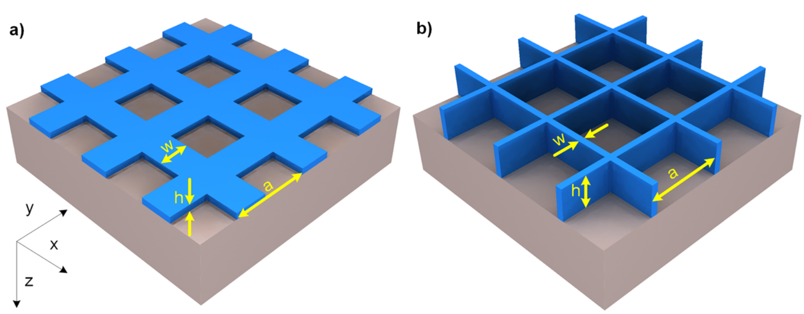

FIG. 1. Geometrical models of (a) *flat* and (b) *tall* AgNW TCFs on the glass substrate. *a*, *w*, and *h* are the lattice constant, width, and height of NWs, respectively.

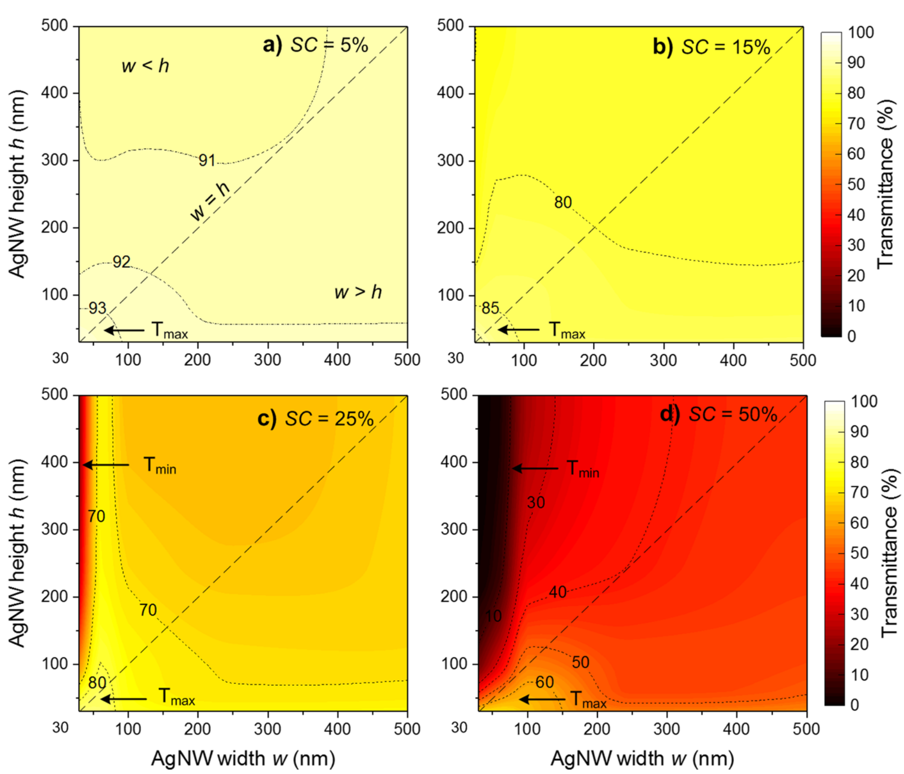

FIG. 2. The average transmittance of AgNW films for the NW width w and height h in the range from 30 to 500 nm, and a) 5%, b) 15%, c) 25%, and d) 50% surface coverage *SC*. The dashed line indicates the AgNWs with $w = h$. Regions T_{max} and T_{min} show the areas of highest and lowest transmittance, respectively.

TABLE I. The aperture width for various w/h and SC. $Aperture\ width = a - w = \frac{w\times(1+\sqrt{1-SC})}{SC} - w$.

w (nm) sc (%)	40	80[c]	250	500
5	1539.7	3079.5	9623.4	19246.8
15	472.5	945	2953.3	5906.5
25	258.6	517.1	1616	3232.1
50	96.6	193.1	603.6	1207.1

Optical haze was evaluated as follows:

$$H = \frac{T_S}{T_T} \tag{1}$$

where T_S is the light scattered from AgNWs into the substrate and T_T is the total light transmitted into the substrate through AgNW film. The forward scattered light was calculated using a total-field scattered-field source, which allows separating the computation region to collect only the scattered field.[34]

Sheet resistance was calculated by percolation model according to Refs. 35 and 36:

$$R_{sh} = \frac{1}{h\sigma_0\left(\phi_f - \phi_{crit}\right)^t}, \tag{2}$$

where σ_0 is the conductivity of metal, ϕ_f is the volume fraction of patterned metal film, ϕ_{crit} is the volume fraction threshold when the patterned film changes from insulator to conductor, h is the thickness of the patterned metal film and t is the critical exponent.

The above-mentioned models were proved to be in good agreement with experimental data and successfully applied by our group in previous works.[37–40]

III. RESULTS AND DISCUSSION

Figure 2 plots the average transmittance of AgNW films with w and h each ranging from 30 to 500 nm, and with 5, 15, 25, and 50% SC. The dashed line indicates the transmittance of AgNWs with a square cross section ($w = h$). NWs with $w = h = 30$ nm reach the maximum transmittance of 95% at SC = 5%, and possess ~ 4, 13, 19 and 25.5% higher transmittance than NWs with $w = h = 500$ nm for 5, 15, 25, and 50% SC respectively. The transmittance above and below dashed line behaves *non-mirror-like*: the flat NWs retain higher T. Flat NWs with SC = 5% show 91.5% average transmittance against 91.1% for tall NWs, while for SC = 15, 25, and 50% this difference becomes larger – 80.4 vs 79.2%, 68.9 vs 65.4%, and 46.3 vs 31.3%. The AgNWs with $w = h \leq 100$ nm (region T_{max} in Fig. 2) exhibit high transmittance due to stronger coupling of the incoming light to surface plasmons at nanoscale dimensions with maximum effect when h is close to metal skin depth (~ 15-50 nm for the Ag/air interface in the visible range).[41–44] The AgNWs with $w \leq 40$ nm, SC = 25% and $w \leq 80$ nm, SC = 50% possess low transmittance for h > 100 nm (region T_{min} in Fig. 2) due to the subwavelength aperture width $a - w$, which is less than 260 nm (see Table I).

Figures 3a and 3b demonstrates the average transmittance and sheet resistance of AgNW films against the ratio of NW width-to-height w/h with the fixed NW cross section area $w\times h$ = 15k nm^2. The transmittance increases with higher w/h ratio – 92, 85, 76, and 57% for w/h = 500/30 vs 90, 74, 40 and 1% for w/h = 30/500 at 5, 15, 25, and 50% SC respectively. The sheet resistance also increases, but by ~ 16.7 times – from few to hundred Ohm/sq, which may significantly affect AgNW performance. This happens due to the decrease of the NW height from 500 to 30 nm (see Eq. 2). To understand how w/h ratio affects both AgNW transmittance and sheet resistance Fig. 3c plots AgNW performance for w/h = 500/30, 250/60, 122.5/122.5, 60/250 and 30/500. AgNW performance increases when w/h ratio lowers, which results in the decrease of the sheet resistance. For example, AgNWs with w/h = 500/30 and 30/500 possess 90% transmittance at 90 and 12 Ohm/sq sheet resistance respectively (see the vertical dashed line in Fig. 3c). Thus, we can claim that tall AgNWs outperform not only flat ones, but even AgNWs with square and circular cross sections. Also, tall AgNWs possess smaller lattice constant useful for some optoelectronics application sensitive to an electron mean free path.[45]

Figure 4 plots the average haze of AgNW films where w and h range from 30 to 500 nm, and for 5, 15, 25, and 50% SC. NWs with

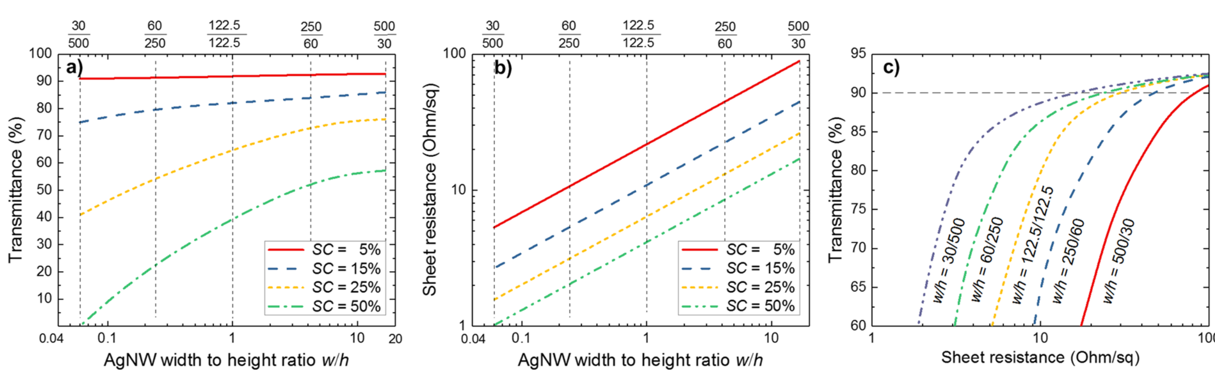

FIG. 3. a) The average transmittance and b) sheet resistance of AgNW films against the ratio of NW width-to-height w/h for surface coverage SC = 5, 15, 25, 50% and the fixed NW cross section area $w\times h$ = 15k nm^2. c) The average transmittance of AgNW films against the sheet resistance for the NW width-to-height ratio w/h = 500/30, 250/60, 122.5/122.5, 60/250, and 30/500.

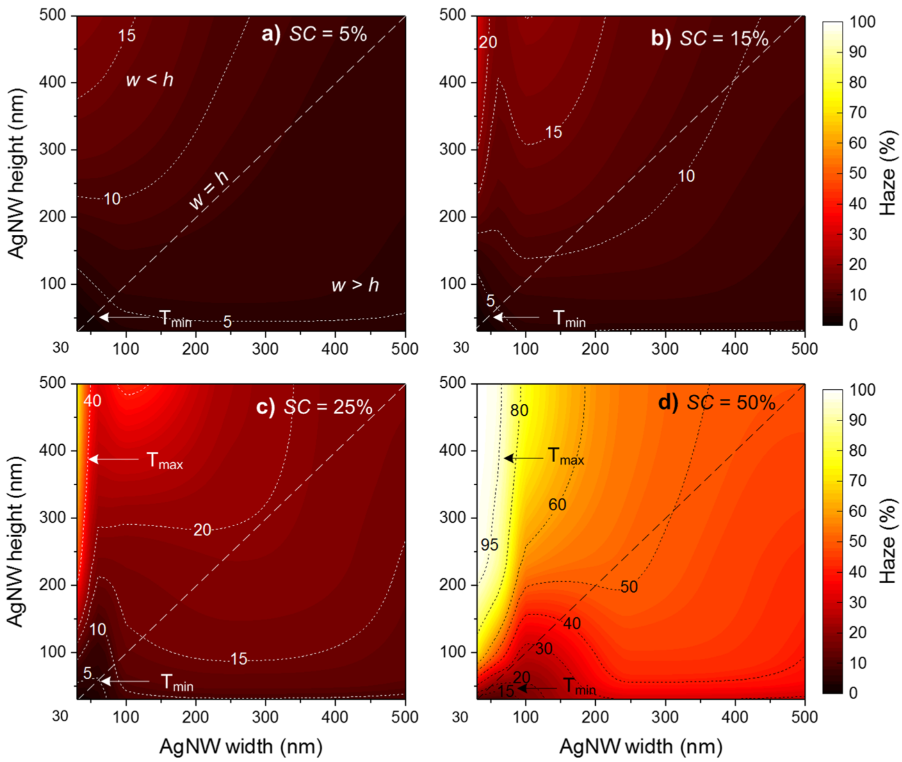

FIG. 4. The average haze of AgNW films for the NW width w and height h ranging from 30 to 500 nm, and a) 5%, b) 15%, c) 25%, and d) 50% surface coverage SC. The dashed line indicates AgNWs with $w = h$.

$w = h = 30$ nm reach the minimum haze of 1% at $SC = 5\%$, and possess ~ 6.5, 8.5, 15 and 38% lower haze than NWs with $w = h = 500$ nm for 5, 15, 25, and 50% SC respectively. Haze above and below dashed line behaves non-mirror-like: the flat NWs retain lower H. Flat NWs with $SC = 5\%$ show 6.5% average haze against 10.3% for tall NWs, while for $SC = 15$, 25, and 50% this difference becomes larger – 8.5 vs 13.3%, 15.5 vs 23.5%, and 42.5 vs 61.8%. AgNWs with $w = h \leq 100$ nm (see region H_{min} on Fig. 4) exhibit lowest haze as a decrease in size of metallic nanostructures reduces the scattering.[46] When w and h increase, AgNWs start to scatter more light with highest H for $h > 100$ nm and the subwavelength aperture width (see region H_{max} on Fig. 4).

Figure 5a demonstrates the average haze of AgNW films against the ratio of NW width-to-height w/h with fixed NW cross section area $w \times h = 15\text{k nm}^2$. The haze increases with lower w/h ratio – 22, 32, 70 and 99% for $w/h = 30/500$ vs 3.5, 5, 9, and 28% for $w/h = 500/30$ at 5, 15, 25, and 50% SC respectively. Thus, AgNWs with $w/h < 1$ definitely suit for thin solar cell applications requiring high H and T, and low R_{sh}. For instance, AgNWs with $w/h = 30/500$ possess $T = 90\%$ at $H = 18\%$ and $R_{sh} = 12$ Ohm/sq, while AgNWs with $w/h = 500/30$ possess same transmittance only at $H = 4.5\%$ and $R_{sh} = 90$ Ohm/sq (see Fig. 5b). In case of application demanding low haze and satisfied by sheet resistance ≥ 100 Ohm/sq (such as touch screens) flat AgNWs are preferable. For other applications requiring

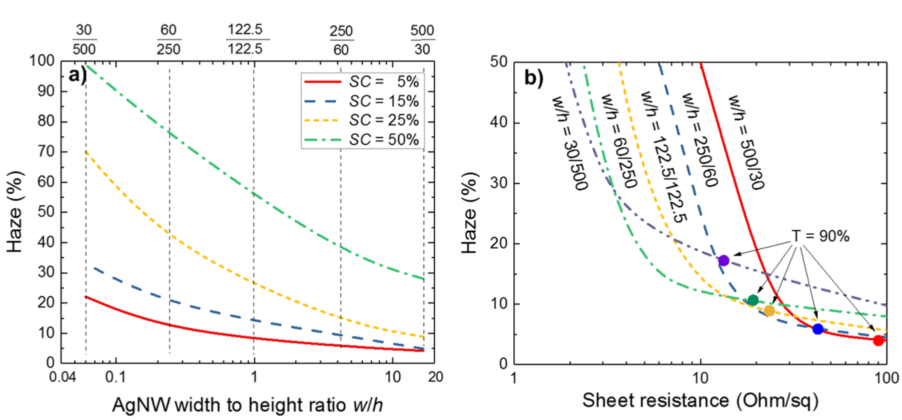

FIG. 5. a) The average haze of AgNW films against the ratio of NW width-to-height w/h for 5, 15, 25 and 50% surface coverage SC ($w \times h = 15\text{k nm}^2$). b) The average haze of AgNW films against the sheet resistance for the NW width-to-height ratio w/h = 500/30, 250/60, 122.5/122.5, 60/250, and 30/500. Colored dots represent $T = 90\%$ for the corresponding curves.

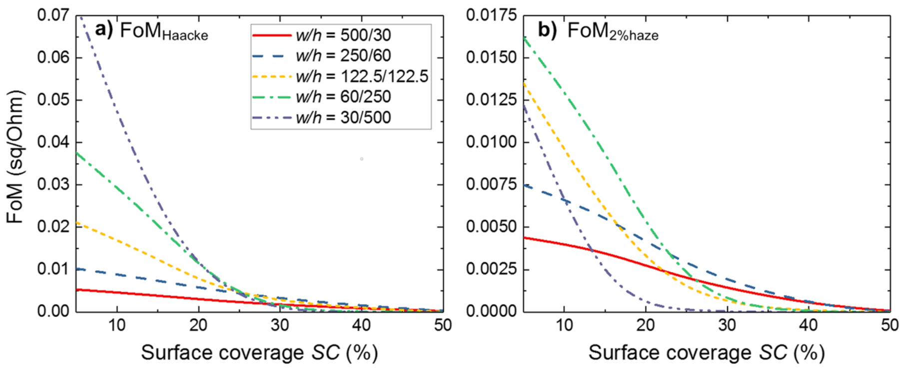

FIG. 6. a) Haacke's *FoM*, and b) $FoM_{2\%haze}$ (T_T = 90%, H = 2%) for various AgNW surface coverage *SC* and width-to-height ratio *w/h*.

low haze and sheet resistance (such as displays), we propose a figure of merit (FoM) enclosing together T, H and R_{sh} and, hence, allowing to estimate the attractiveness of AgNW TCFs for broad range of applications. In 1972 D.B. Fraser and H.D. Cook first proposed the following equation for FoM of the TCFs:[47]

$$FoM = \frac{T}{R_{sh}} \tag{3}$$

Several years later G. Haacke showed that the maximum *FoM* in Eq. 3 corresponds to T = 37%, which is not satisfactory for most optoelectronic applications.[48] G. Haacke modified the Eq. 3 as follows:

$$FoM = \frac{T^x}{R_{sh}} \tag{4}$$

where he set x equal to 10 in order to fit the maximum *FoM* for T = 90%. Noteworthy, such modification is accurate only for the case when $R_{sh} \geq 1$ Ohm/sq: for example, T = 90% and R_{sh} = 5 Ohm/sq results in two times lower *FoM* – 0.0697 sq/Ohm, than T = 65% and R_{sh} = 0.1 Ohm/sq – 0.1346 sq/Ohm.

Here we propose a further update of the Eq. 4 considering the optical haze:

$$FoM = \frac{T_F^x}{R_{sh}} \tag{5}$$

where T_F is the forward transmitted light into substrate through AgNWs and equals to:

$$T_F = T_T - T_S = T_T(1 - H) \tag{6}$$

The total transmittance is given by $T_T = \exp(-\alpha h)$, where α is the optical absorption coefficient and h is the thickness of TCF. The value $(1 - H)$ corresponds to the reduction in the total transmittance due to the haze and can be evaluated as $\exp(-\beta h)$, where β is the optical haze-related coefficient. According to above-mentioned expressions, we can rewrite Eq. 5 as follows:

$$FoM = \frac{e^{-hx(\alpha+\beta)}}{R_{sh}} \tag{7}$$

After deriving Eq. 7 and then equating it to zero, we achieve a maximum value at $h_{max} = [x(\alpha+\beta)]^{-1}$. Substituting h_{max} into $T_F = \exp[-h(\alpha+\beta)]$ we obtain $T_F = \exp(-1/x)$. After merging Eq. 5 and 6 we find expression for x:

$$x = -\frac{1}{\ln[T_T(1 - H)]} \tag{8}$$

For T_T = 90% and H = 0 we obtain Haacke's *FoM* with x = 10. For T_T = 90% and H = 2% x becomes equal to 7.96. Figure 6a plots Haacke's *FoM* for various surface coverage *SC*, where tallest NWs possess the highest performance, which agrees with Fig. 3c. Different behavior is observed for $FoM_{2\%haze}$ (x = 7.96): AgNWs with w/h = 60/250 show up to 1.2 times higher value than AgNWs with other ratios (see Fig. 6b). Indeed, AgNWs with w/h = 60/250 offer attractive T_T, R_{sh} and H parameters: 91.5%, 10 Ohm/sq and 10% respectively (see Table II). For more sensitive display applications AgNWs with w/h = 122.5/122.5 and w/h = 250/60 can be selected as well, possessing lower H (5÷7%) at the cost of higher R_{sh} (21÷45 Ohm/sq). Worth to mention, Haacke's *FoM* matches the situation where high haze of the rectangular shaped AgNWs is demanded.

Figure 7 shows the transmittance, sheet resistance and haze of AgNW films with fixed *SC* = 5% against the various NW cross section area $w\times h$ and width-to-height ratio *w/h*. The white solid curve indicates the maximum value of Haacke's *FoM* for each cross-section area appearing at the lowest ratio w/h = 30/500. When NW cross-section area increases from 5k to 25k nm^2, AgNW transmittance decreases insignificantly – ~1%, while the sheet resistance reduces from 8 to 4 Ohm/sq and haze raises from 13 to 25% resulting in further increase of AgNW performance for thin solar cell applications. The white dashed curve shows the maximum value of $FoM_{2\%haze}$ appearing at ratios w/h = 0.15÷0.35 retaining T, R_{sh} and H within 90÷91.5%, 6÷15 Ohm/sq and 15÷8% respectively.

TABLE II. Optical properties of AgNWs with various ratio *w/h* and *SC* = 5%.

Opt. props. *w/h*	T_T (%)	R_{sh} (Ohm/sq)	H (%)	FoM_{Haacke} (sq/Ohm)	$FoM_{2\%haze}$ (sq/Ohm)
30/500	90.9	5.3	22	0.072	0.0122
60/250	91.2	10.6	12	0.037	0.0162
122.5/122.5	91.8	20.1	7.5	0.021	0.0135
250/60	92	45	5	0.01	0.0075
500/30	92.5	90	4	0.005	0.004

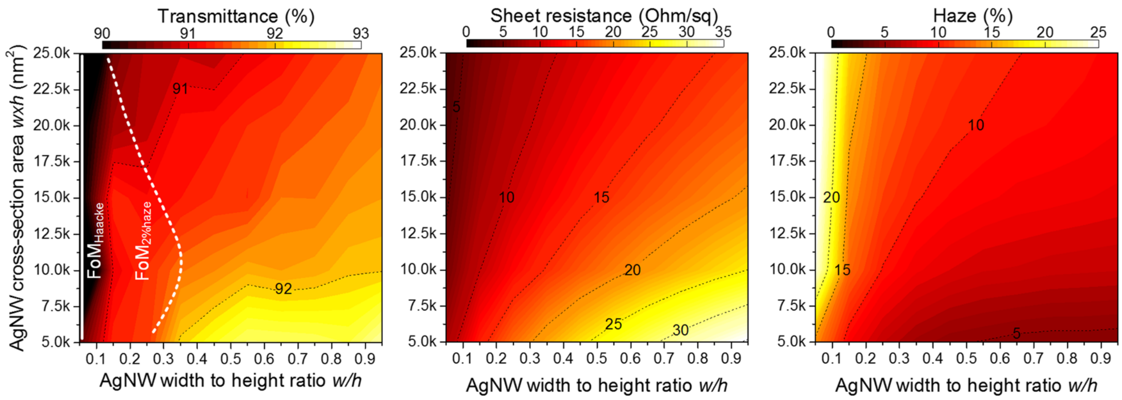

FIG. 7. The transmittance, sheet resistance and haze of AgNW films with fixed *SC* = 5% for the various NW cross-section area $w \times h$ and width-to-height ratio *w/h*. The white solid and dashed lines indicate the maximum values of Haacke's *FoM* and $FoM_{2\%haze}$ for each cross-section area.

IV. CONCLUSION

TCFs based on rectangularly shaped AgNWs with different width-to-height ratios were theoretically investigated. Tall AgNWs demonstrates higher transmittance and optical haze and lower sheet resistance compared to flat AgNWs makings them a transparent conductive film of choice for thin solar cell applications. We propose an update for Haacke's figure of merit to enclose haze factor, which can be used to find performance trade-off for broader range of applications including those, which require low haze. Obtained results grant an opportunity for deeper analysis of AgNW properties for many optoelectronic applications.

ACKNOWLEDGMENTS

A.S. would like to thank the support from A. Kladov, director of BAS Innovation Ltd. (Minsk, Belarus); State Programs of Scientific Research of the Republic of Belarus «Physical Materials Science, New Materials and Technologies» (2.45) and «Convergence-2020» (3.03).

X.W.S. would like to thank the support from the National Key Research and Development Program of China administrated by the Ministry of Science and Technology of China (No. 2016YFB0401702); National Natural Science Foundation of China (No. 61674074 and 61405089), Shenzhen Peacock Team Project (No. KQTD2016030111203005); Shenzhen Innovation Project (No. JCYJ20160301113356947, JCYJ20160301113537474); Shenzhen Key Lab of Advanced Quantum Dot Displays and Lighting, and Guangdong Higher Education Key Lab of Advanced Quantum Dot Displays and Lighting.

REFERENCES

[1] D. Langley, G. Giusti, C. Mayousse, C. Celle, D. Bellet, and J.-P. Simonato, Nanotechnology **24**, 452001 (2013).
[2] S. De, T. M. Higgins, P. E. Lyons, E. M. Doherty, P. N. Nirmalraj, W. J. Blau, J. J. Boland, and J. N. ColemanACS, Nano **3**, 1767 (2009).
[3] K. Ellmer, Nat. Photonics **6**, 809 (2012).
[4] D. S. Hecht, L. Hu, and G. Irvin, Adv. Mater. **23**, 1482 (2011).
[5] L. Hu, H. Wu, and Y. Cui, MRS Bull. **36**, 760 (2011).
[6] C. P. Muzzillo, Sol. Energy Mater. Sol. Cells **169**, 68 (2017).
[7] W. He and C. Ye, J. Mater. Sci. Technol. **31**, 581 (2015).
[8] L. He and S. C. Tjong, Mater. Sci. Eng. R Rep. **109**, 1 (2016).
[9] K. Ghaffarzadeh and R. Das, *Transparent Conductive Films and Materials 2018-2028: Forecasts, Technologies, Players* (IDTechEx Research, 2018).
[10] J. H. Maurer, L. González-García, B. Reiser, I. Kanelidis, and T. Kraus, Nano Lett. **16**, 2921 (2016).
[11] C. J. Emmott, A. Urbina, and J. Nelson, Sol. Energy Mater. Sol. Cells **97**, 14 (2012).
[12] D. S. Hecht and R. B. Kaner, MRS Bull. **6**, 749 (2011).
[13] J.-Y. Lee, S. T. Connor, Y. Cui, and P. Peumans, Nano Lett. **8**, 689 (2008).
[14] B. Azzopardi, C. J. M. Emmott, A. Urbina, F. C. Krebs, J. Mutale, and J. Nelson, Energy Environ. Sci. **4**, 3741 (2011).
[15] S. Nam, M. Song, D. H. Kim, B. Cho, H. M. Lee, J. D. Kwon, S. G. Park, K. S. Nam, Y. Jeong, S. H. Kwon, Y. C. Park, S. H. Jin, J. W. Kang, S. Jo, and C. S. Kim, Sci. Rep. **4**, 4788 (2014).
[16] D.-H. Kim, K.-C. Yu, Y. Kim, and J.-W. Kim, ACS Appl. Mater. Interfaces **7**, 15214 (2015).
[17] L. Yang, T. Zhang, H. Zhou, S. C. Price, B. J. Wiley, and W. You, ACS Appl. Mater. Interfaces **3**, 4075 (2011).
[18] L. Hu, H. S. Kim, J.-Y. Lee, P. Peumans, and Y. Cui, ACS Nano **4**, 2955 (2010).
[19] C. Mayousse, C. Celle, E. Moreau, J.-F. Mainguet, A. Carella, and J.-P. Simonato, Nanotechnology **24**, 215501 (2013).
[20] J. Jung, H. Lee, I. Ha, H. Cho, K. K. Kim, J. Kwon, P. Won, S. Hong, and S. H. Ko, ACS Appl. Mater. Interf. **9**, 44609 (2017).
[21] P. Lee, J. Ham, J. Lee, S. Hong, S. Han, Y. D. Suh, S. E. Lee, J. Yeo, S. S. Lee, and S. H. Ko, Adv. Funct. Mater. **24**, 5671 (2014).
[22] S. Hong, H. Lee, J. Lee, J. Kwon, S. Han, Y. D. Suh, H. Cho, J. Shin, J. Yeo, and S. H. Ko, Adv. Mater. **27**, 4744 (2015).
[23] H. Moon, P. Won, J. Lee, and S. H. Ko, Nanotechnology **27**, 295201 (2016).
[24] Y. D. Suh, S. Hong, J. Lee, H. Lee, S. Jung, J. Kwon, H. Moon, P. Won, J. Shin, J. Yeo, and S. H. Ko, RSC Advances **6**, 57434 (2016).
[25] S. Jang, W. B. Jung, C. Kim, P. Won, S. G. Lee, K. M. Cho, M. L. Jin, C. J. An, H. J. Jeon, S. H. Ko, T. S. Kim, and H. T. Jung, Nanoscale **8**, 14257 (2016).
[26] S. Hong, J. Yeo, G. Kim, D. Kim, H. Lee, J. Kwon, H. Lee, P. Lee, and S. H. Ko, ACS Nano **7**, 5024 (2013).
[27] C. Preston, Y. Xu, X. Han, J. N. Munday, and L. Hu, Nano Res. **6**, 461 (2013).
[28] M. Marus, A. Hubarevich, W. J. Fan, H. Wang, A. Smirnov, K. Wang, H. Huang, and X. W. Sun, AIP Adv. **8**, 035201 (2018).
[29] H. Moon, P. Won, J. Lee, and S. H. Ko, Nanotechnology **27**, 295201 (2016).
[30] C. Chen, Y. Zhao, W. Wei, J. Tao, G. Lei, D. Jia, M. Wan, S. Li, S. Ji, and C. Ye, J Mater Chem C **5**, 2240 (2017).
[31] C. Preston, Z. Fang, J. Murray, H. Zhu, J. Dai, J. N. Munday, and L. Hu, J Mater Chem C **2**, 1248 (2014).

[32]Lumerical Solutions, Inc., https://www.lumerical.com/products/fdtd-solutions/.
[33]E. D. Palik, *Handbook of optical constants of solids*, 3 (Nachdr. Acad. Press, San Diego, Calif, 2003).
[34]Lumerical Solutions, Inc., https://kb.lumerical.com/ref_sim_obj_sources_tfsf.html.
[35]B. J. Last and D. J. Thouless, Phys. Rev. Lett. **27**, 1719 (1971).
[36]J. P. Fitzpatrick, R. B. Malt, and F. Spaepen, Phys. Lett. A **47**, 207 (1974).
[37]M. Marus, A. Hubarevich, R. J. W. Lim, H. Huang, A. Smirnov, H. Wang, W. Fan, and X. W. Sun, Opt. Mater. Express **7**, 1105 (2017).
[38]A. Hubarevich, M. Marus, W. Fan, A. Smirnov, X. W. Sun, and H. Wang, Opt. Express **23**, 17860 (2015).
[39]M. Marus, A. Hubarevich, H. Wang, A. Stsiapanau, A. Smirnov, X. W. Sun, and W. Fan, Opt. Express **23**, 26794 (2015).
[40]M. Marus, A. Hubarevich, H. Wang, A. Smirnov, X. Sun, and W. Fan, Opt. Express **23**, 6209 (2015).
[41]W. L. Barnes, A. Dereux, and T. W. Ebbesen, Nature **424**, 824 (2003).
[42]H. Raether, *Surface Plasmons on Smooth and Rough Surfaces and on Gratings*, 111 (Springer Berlin Heidelberg, 1988), p. 91.
[43]J. Homola and M. Piliarik, *Surface Plasmon Resonance Based Sensors*, 4 (Springer Berlin Heidelberg, 2006), p. 45.
[44]K. Azad and W. Zhang, Opt. Lett. **30**, 2945 (2005).
[45]A. Kumar, J. Appl. Phys. **121**, 014502 (2017).
[46]P. K. Jain, K. S. Lee, I. H. El-Sayed, and M. A. El-Sayed, J. Phys. Chem. B **110**, 7238 (2006).
[47]D. B. Fraser and H. D. Cook, J. Electrochem. Soc. **119**, 1368 (1972).
[48]G. Haacke, J. Appl. Phys. **47**, 4086 (1976).